Jinst

Published by IOP Publishing for Sissa Medialab

Received: *December 14, 2017*
Accepted: *January 26, 2018*
Published: *February 13, 2018*

XII International Symposium on Radiation from Relativistic Electrons in Periodic Structures — RREPS-17
18–22 September, 2017
DESY, Hamburg, Germany

Mass dependence of spectral and angular distributions of Cherenkov radiation from relativistic isotopes in solid radiators and its possible application as mass selector

O.V. Bogdanov,[a,b] **E.I. Rozhkova,**[a,1] **Yu.L. Pivovarov and N. Kuzminchuk-Feuerstein**[c]

[a] *National Research Tomsk Polytechnic University, 634050 Lenin Ave. 30, Tomsk, Russia*
[b] *National Research Tomsk State University, 634050 Lenin Ave. 36, Tomsk, Russia*
[c] *GSI Helmholtzzentrum für Schwerionenforschung, 64291 Darmstadt, Germany*

E-mail: elenafiks@gmail.com

Abstract: The first proof of principle experiment with a prototype of a Time-of-Flight (TOF) - Cherenkov detector of relativistic heavy ions (RHI) exploiting a liquid Iodine Naphthalene radiator has been performed at Cave C at GSI (Darmstadt, Germany). A conceptual design for a liquid Cherenkov detector was proposed as a prototype for the future TOF measurements at the Super-FRS by detection of total number of Cherenkov photons. The ionization energy loss of RHI in a liquid radiator decreases only slightly this number, while in a solid radiator changes sufficiently not the total number of ChR photons, but ChR angular and spectral distributions. By means of computer simulations, we showed that these distributions are very sensitive to the isotope mass, due to different stopping powers of isotopes with initial equal relativistic factors. The results of simulations for light (Li, Be) and heavy (Xe) isotopes at 500–1000 MeV/u are presented indicating the possibility to use the isotopic effect in ChR of RHI as the mass selector.

Keywords: Cherenkov and transition radiation; Instrumentation for heavy-ion accelerators; Liquid detectors; Solid state detectors

[1] Corresponding author.

https://doi.org/10.1088/1748-0221/13/02/C02015

Contents

2018 JINST 13 C02015

1 Introduction

The new Super-Fragment Separator [1, 2] (Super-FRS) at the FAIR GSI (Darmstadt, Germany) in a wide range of ions with energies up to 1.5 AGeV will be used for the production of isotopes by projectile fragmentation and fission. In order to separate and identify fragmentation products a high resolving power detector system is required for position and Time-Of-Flight (TOF) measurements. A high performance TOF detector is one of the key detectors to measure the velocity and mass of the particles. The first proof of principle experiment with Cherenkov TOF detector of relativistic heavy ions (RHI) exploiting a liquid Iodine Naphthalene radiator has been performed at Cave C at GSI [3]. The new Cherenkov TOF detector is based on registration of light (Cherenkov photons) emitted in liquid. Along with a total number of ChR (Cherenkov radiation) photons, in case of optically transparent solid radiators additional applications of ChR arise for instrumentation for heavy-ion accelerators, connected with the measurements of ChR spectral and angular distributions.

The spectral-angular distributions of Cherenkov radiation (ChR) from relativistic heavy ions (RHI) with account of energy loss in solid radiators show complicated diffraction-like structures, see [4, 5] and references therein, which differ from Tamm-Frank [6] distributions. The width and shape of these structures depend on the mean ionization energy loss, which depends on the RHI mass through the maximum energy transfer in a single collision [7]. Thus, in case of isotopes entering the solid radiator with equal relativistic factor, the positions of ChR maximums depend on their masses (called the isotopic effect in ChR from RHI [8]). Besides the pure physical interest, the predicted isotopic effect can be considered as the new tool for isotopes mass determination (mass selector), similar to Cherenkov light detection as a velocity selector for uranium fission products at intermediate energies, presented in [9].

2 ChR from RHI in liquid radiator

In many RHI experiments gaseous or solid materials are commonly used as Cherenkov radiators for particle identification and energy measurements [10, 11]. The circulation of gaseous or liquid

active materials allows regular refreshing and can greatly reduce the performance degradation due to ageing after exposure to high ion rates. Other advantages of fluid over TOF systems based on solid-state materials, including small area diamond or silicon are the virtually unlimited radiation hardness of the fluid (through recirculation or replacement), and the relative simplicity of the readout electronics based on photomultiplier tubes [3].

Typical refractive indices of a gaseous Cherenkov radiators are around $n = 1.0003$ (corresponding Cherenkov thresholds around $\beta = 0.99$). This is inapplicable for the future measurements at SuperFRS, where one will need to cope also with lowest primary particle energies of ~ 200 MeV/u, with a corresponding Cherenkov threshold of $\beta = 0.59$, requiring a radiator refractive index of around $n = 1.7$. For a future TOF detector based on liquid radiator, e.g. an Iodine Naphthalene liquid ($C_{10}H_7I$) is proposed [3]. The high refractive index if this liquid of $n = 1.70003$ at 589 nm and its nevertheless relatively low density of $\rho = 1.738\,\mathrm{g/cm^2}$ makes it suitable for a continuous flow of the material [3].

The number of Cherenkov photons emitted during the penetration of an ion with a charge Z in an optical spectral range $\lambda_1 \div \lambda_2$ is estimated according to the standard formulae based on the Tamm-Frank theory [6]:

$$\frac{dN_{\mathrm{Ch}}}{d\lambda dx} = \frac{2\pi}{137} Z^2 \left(1 - \frac{1}{n(\lambda)^2 \beta_0^2}\right) \frac{1}{\lambda^2} \tag{2.1}$$

where dx is the radiator thickness and β_0 the initial ion velocity. This theory ignores decreasing of RHI velocity due to ionization energy loss. Authors [5] established a more refined approach, which includes the calculation of the energy loss and decrease of RHI velocity depending on penetration depth in the solid radiator. In the calculations the thickness of the radiator L is divided into N number of segments and the energy loss at each segment length $\Delta x = L/N$ may be calculated using the modern packages SRIM 2013 [12] or ATIMA [13]. The number of Cherenkov photons is then equal to

$$N_{\mathrm{Ch-Stopping}} = \sum_{i=1}^{N} \frac{dN_{\mathrm{Ch}}(\beta_i)}{d\lambda dx} \Delta x \tag{2.2}$$

where β_{i} is calculated for each segment of length Δx.

To illustrate the role of RHI energy loss in a liquid radiator, the Cherenkov photon density $dN_{\mathrm{Ch}}/d\lambda$ as a function of wavelength is plotted in figure 1 according to the Tamm-Frank theory and including the RHI energy loss. The calculations are shown for nickel and xenon ions with energies of 234 MeV/u, 323 MeV/u and 600 MeV/u, respectively as it was during the online measurements at CaveC at GSI in April 2014 [3].

As one can see, the RHI energy loss in a liquid radiator only slightly decreases the total number of Cherenkov photon density. In the section 3 and 4 we will show the essential sensitivity of the differential characteristics of ChR to the energy loss of RHI in solid radiators.

3 ChR from RHI in solid radiator — qualitative consideration

The first measurements of the Cherenkov radiation (ChR) angular distributions from RHI with the present FRS have revealed that the well known Tamm-Frank theory cannot describe the observed results [14–16]. The new models [4, 5] predict that at the FRS and Super-FRS energies the

2018 JINST 13 C02015

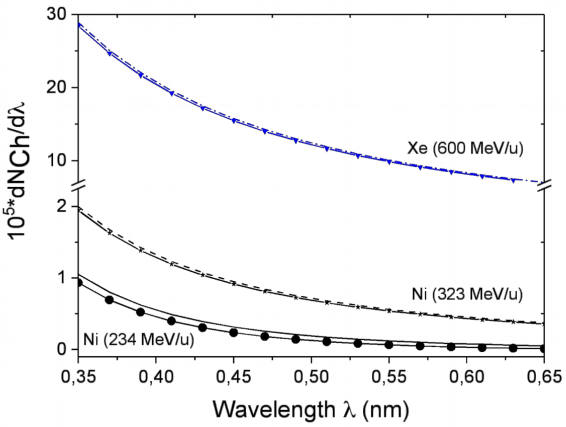

Figure 1. Calculated Cherenkov photon density $dN_{\mathrm{Ch}}/d\lambda$ (eq. (2.2)) as a function of wavelength for ^{58}Ni and ^{124}Xe ions: solid lines — calculations based on the Tamm-Frank theory; line + symbol — calculations including the energy loss of RHI in the liquid radiator. The energies of RHI are chosen like in the experiment [3].

energy loss of the ions in the radiator leads to broadening and appearing of the complex diffraction structures of the spectral and angular distributions. These distributions are very sensitive to the charge and velocity of RHI and radiator thickness [5, 8], thus the experiments with the Super-FRS will contribute to the detailed understanding of ChR from RHI ions and will lay the ground for improved and novel detector developments, like velocity selector [9].

Cherenkov radiation appears when the particle velocity is greater than the phase velocity of light in matter: $v/c = \beta > 1/n(\omega)$, where $n(\omega)$ and β — are the refraction index of the radiator and RHI velocity, respectively. The ChR emission angle ϑ is defined by the condition: $\cos\vartheta > 1/\beta\, n(\omega)$. The spectral-angular distribution of ChR is (see e.g. [7]):

$$\frac{d^2W}{d\omega d\Omega} = \frac{(Ze\sin\theta)^2\,\omega^2}{4\pi^2c^3} n(\omega)\left|\int_0^L \exp\left[i\omega\left(t(x) - n(\omega)\frac{x\cos\theta}{c}\right)\right]dx\right|^2. \tag{3.1}$$

Here: c is the speed of light in vacuum, Ze is the RHI charge; $t(x) = \int_0^x \frac{dy}{v(y)}$ is the RHI time-of-flight through radiator depending on its velocity $v(x)$ that decreases due to slowing down and L is the thickness of the radiator.

The slowing-down is very complicated function of RHI energy. We shall consider the ChR from 500–1000 GeV/u (GSI and FAIR energies) RHI when for qualitative analysis one can use the Bethe-Bloch formula, and for more precise numerical calculations the computer codes SRIM 2013 (Ziegler) [12] or ATIMA (H. Weick) [13]. The relativistic Bethe-Bloch formula for mean ionization energy loss reads [7]:

$$\left\langle -\frac{dE}{dx}\right\rangle = kZ^2\frac{Z_t}{A_t}\frac{1}{\beta^2}\left[\frac{1}{2}\ln\frac{2m_ec^2\beta^2W_{\max}}{I^2} - \beta^2 - \frac{\delta(\beta\gamma)}{2}\right], \tag{3.2}$$

where $k = 0.307075\,\mathrm{MeVg^{-1}cm^2}$, I is the mean excitation energy, Z_t and A_t are the atomic number and atomic mass of radiator, $\delta(\beta\gamma)$ is the density effect correction to ionization energy loss. The

2018 JINST 13 C02015

Bethe-Bloch formula contains projectile charge squared and mass dependence through $W_{\max}$. The Z^2 dependence leads to a huge increase of ChR photon number compared to electrons and protons. The RHI mass enters the equation for the maximal energy transfer to a target electron:

$$W_{\max} = \frac{2m_e c^2 \beta^2 \gamma^2}{1 + 2\gamma m_e/M + (m_e/M)^2}. \tag{3.3}$$

As in [8], let two isotopes with different masses M_1 and M_2 have equal initial relativistic factors $\gamma_0 = \gamma_1(0) = E_1(0)/\left(M_1 c^2\right) = \gamma_2(0) = E_2(0)/\left(M_2 c^2\right)$, but after penetration through a thin layer of radiator Δx, as it follows from eqs. (3.2)–(3.3), the isotopes **loose different amount of energy** and enter the next piece of the radiator with the energies:

$$\begin{aligned} E_1(\Delta x) &= E_1(0) - \Delta E_1 \Delta x = E_1(0) - S_1(\gamma_0) \cdot \Delta x, \\ E_2(\Delta x) &= E_2(0) - \Delta E_2 \Delta x = E_2(0) - S_2(\gamma_0) \cdot \Delta x. \end{aligned} \tag{3.4}$$

Here, $S(\gamma) = -dE/dx$ is the stopping power. Assuming $E_1(0) \neq E_2(0)$, the relativistic factors of isotopes after penetration depth Δx become different:

$$\gamma_1(\Delta x) = \frac{E_1(\Delta x)}{M_1 c^2} = \gamma_0 - \frac{S_1(\gamma_0) \cdot \Delta x}{M_1 c^2}; \quad \gamma_2(\Delta x) = \frac{E_2(\Delta x)}{M_2 c^2} = \gamma_0 - \frac{S_2(\gamma_0) \cdot \Delta x}{M_2 c^2} \tag{3.5}$$

In view of eqs. (3.4)–(3.5), the ratio of relativistic factors becomes equal to:

$$\frac{\gamma_1(\Delta x)}{\gamma_2(\Delta x)} = \frac{1 - S_1(\gamma_0) \cdot \Delta x/\gamma_0 M_1 c^2}{1 - S_2(\gamma_0) \cdot \Delta x/\gamma_0 M_2 c^2} = \frac{1 - \xi_1}{1 - \xi_2}. \tag{3.6}$$

As it follows from the eq. (3.6), the ratio of quantities

$$\frac{\xi_1}{\xi_2} = \frac{S_1(\gamma_0)}{S_2(\gamma_0)} \cdot \frac{M_2}{M_1} \tag{3.7}$$

depends on isotopes mass ratio, even if the stopping powers differ not much. By calculating $\gamma(\Delta x)$ values, one can obtain the velocity values at all penetration depths, substitute them into eq. (3.1) and provide further numerical calculations of ChR spectral-angular distributions.

4 ChR from RHI in solid radiator — simulations of isotopic effect

The further consideration is based on numerical calculations using eq. (3.1) and the slowing-down of RHI, calculated with ATIMA [13] package that allows to obtain exact values of the RHI energy as it penetrates through radiator. The figures 2–4 present the spectral-angular distributions of ChR from Li, Be and Xe isotopes. The broadening is clearly seen and, in accordance with (9), is more brilliant for light isotopes, when the difference in masses (almost twice) plays the key role.

The dramatic change in ChR spectra from Li (figure 2) to Be (figure 3) isotopes is due to the different radiator thickness (in figure 3 it is twice as large as in figure 2) and initial isotopes energy (in figure 3 for Be it is half of that for Li in figure 2). As a sequence, the influence of slowing-down on the ChR spectra is more remarkable in figure 3. Since the Cherenkov radiation angle is connected with isotope velocity, which decreases due to slowing-down, and due to interference of

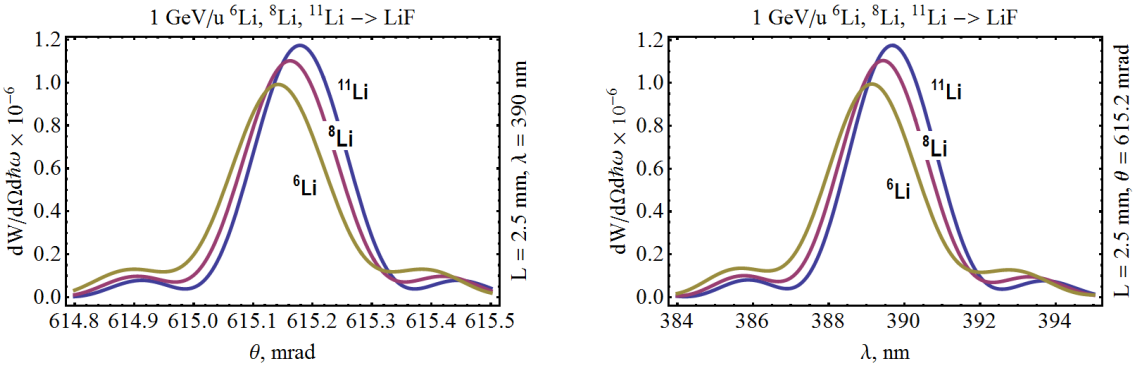

Figure 2. Angular (left) and spectral (right) distributions of Cherenkov radiation from lithium isotopes (^{6}Li, ^{8}Li, ^{11}Li) at 1 GeV/u in LiF radiator. The radiator thickness $L = 2.5$ mm. For angular distributions LiF refractive index equals 1.39958 (at 390 nm), for spectral distributions it changes from 1.39996 to 1.39926 (384–395 nm).

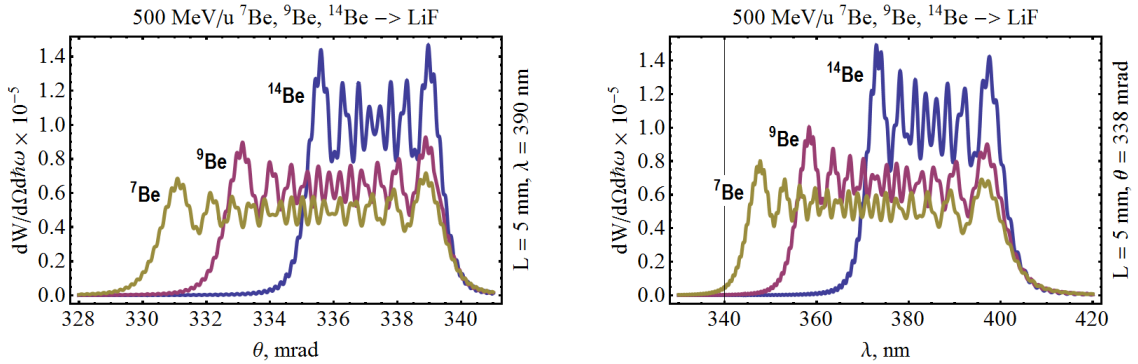

Figure 3. Angular (left) and spectral (right) distributions of Cherenkov radiation from beryllium isotopes (^{7}Be, ^{9}Be, ^{14}Be) at 500 MeV/u in LiF. The radiator thickness $L = 5$ mm. For angular distributions LiF refractive index equals 1.39958 (at 390 nm), for spectral distributions it changes from 1.4048 to 1.39778 (330–420 nm).

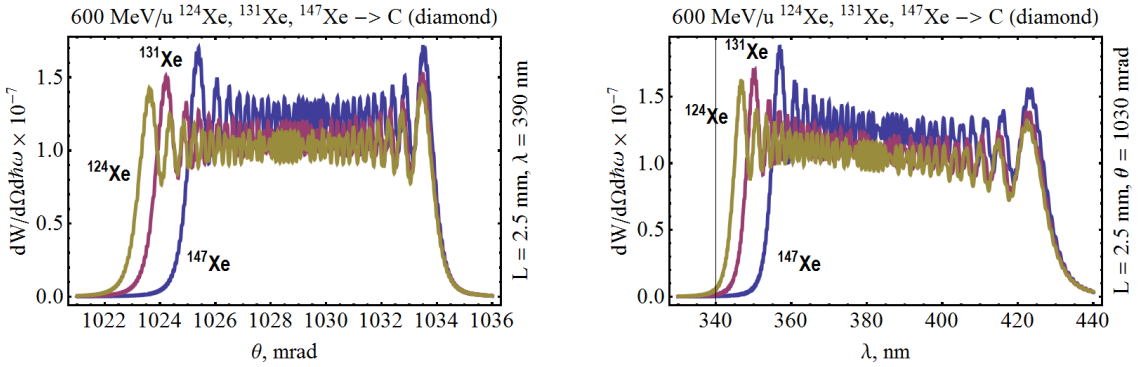

Figure 4. Angular (left) and spectral (right) distributions of Cherenkov radiation from uranium isotopes (^{124}Xe, ^{131}Xe, ^{147}Xe) at 600 MeV/u in diamond radiator. The radiator $L = 2.5$ mm. For angular distributions diamond refractive index equals 2.4688 (at 390 nm), for spectral distributions it changes from 2.5088 to 2.4485 (330–420 nm).

2018 JINST 13 C02015

waves emitted from different parts of isotope trajectory many peaks ("diffraction-like structure") appear in both spectral and angular distributions.

One may suggest that the presented results can be used as isotopes mass selector, due to differences among isotopes spectra, even they are always continuous and overlapped. The possible solution is the sensibility of the FWHM of calculated spectra to the isotope mass. The "overlapping" problem is under study and the results will be published in a separate paper.

5 Conclusions

The future TOF measurements at the Super-FRS will be based on the detection of total number of Cherenkov photons from RHI in a liquid radiator. The ionization energy loss of RHI in a liquid radiator only slightly decreases the total number of Cherenkov photons. Recently a first ring-imaging Cherenkov counter for heavy ions (HI-RICH) was developed [17] and demonstrated its great advantages compared to conventional TOF detectors. Our results may contribute to improvement of Monte-Carlo procedure [17] based on Tamm-Frank formula, i.e. how to consider in a more correct way the influence of relativistic heavy ions (isotopes) energy loss in a radiator on Cherenkov photon number.

We showed by means of computer simulations that the ionization energy loss of RHI in a solid radiator changes sufficiently not the total number of ChR photons, but ChR angular and spectral distributions. There also arises the specific difference of these distributions for RHI with the same charge but different masses — the isotopic effect in ChR. The first estimations of the isotopic effect in RHI ChR [8] revealed that for the fixed ChR wave length the diffraction maximums in ChR angular distributions for different isotopes are shifted relative to each other. The simulated ChR spectral distributions (fixed observation angle) from light and heavy (Li, Be, Xe) 500–1000 MeV/u isotopes in diamond and LiF solid radiators clearly show that they also are well sensitive to the isotope mass (if the incident relativistic factor is the same). The predicted isotopic effects in spectral-angular distributions of ChR from RHI in transparent solid radiators probably can be used as isotopes mass selector, similar to Cherenkov light detection as a velocity selector for uranium fission products at intermediate energies [9].

Acknowledgments

The authors thank Prof. Dr. H. Geissel and Prof. Dr. C. Scheidenberger for numerous discussions on Cherenkov radiation from RHI. This work contributes to Scientific Program of the Super-FRS Experiment Collaboration [18]. The research is carried out at GSI Darmstadt and at TPU Tomsk within the framework of Tomsk Polytechnic University Competitiveness Enhancement Program.

References

[1] H. Geissel et al., *The Super-FRS project at GSI*, *Nucl. Instrum. Meth.* **B 204** (2003) 71.

[2] O. Klepper et al., *First steps towards radioactive beams in the experimental storage rings at GSI*, *Nucl. Instrum. Meth.* **B 70** (1992) 427.

2018 JINST 13 C02015

[3] N. Kuzminchuk-Feuerstein, N. Ferber, E. Rozhkova, I. Kaufeld and B. Voss, *First beam test of a liquid Cherenkov detector prototype for a future TOF measurements at the Super-FRS*, Nucl. Instrum. Meth. **A 866** (2017) 207.

[4] E.S. Kuzmin and A.V. Tarasov, *Diffraction like effects in angular distribution of Cherenkov radiation from heavy ions*, *JINR Rapid Commun.* **4-61-93** (1993) 64.

[5] E.I. Rozhkova and Yu.L. Pivovarov, *Mixed optical Cherenkov-Bremsstrahlung radiation in vicinity of the Cherenkov cone from relativistic heavy ions: Unusual dependence of the angular distribution width on the radiator thickness*, *Phys. Lett.* **A 380** (2016) 2386.

[6] I.E. Tamm and I.M. Frank, *Kogerentnoe izlučenie bystrogo elektrona v srede*, *Dokl. Akad. Nauk SSSR* **14** (1937) 107.

[7] Particle Data Group, C. Patrignani et al., *Review of Particle Physics*, *Chinese Phys.* **C 40** (2016) 100001.

[8] O.V. Bogdanov and Yu.L. Pivovarov, *Angular Distributions of Cherenkov Radiation from Relativistic Heavy Ions: Stopping and Isotopic Effects*, *Nuovo Cim.* **34** (2011) 103.

[9] T. Yamaguchi et al., *Cherenkov light detection as a velocity selector for uranium fission products at intermediate energies*, Nucl. Instrum. Meth. **A 766** (2014) 123.

[10] A. Margaryan, O. Hashimoto, S. Majewski and L. Tang, *RF Cherenkov picosecond timing technique for high energy physics applications*, Nucl. Instrum. Meth. **A 595** (2008) 274.

[11] J. Va'vra, C. Ertley, D.W. G.S. Leith, B. Ratcliff and J. Schwiening, *A High-resolution TOF Detector: A Possible Way to Compete with a RICH Detector*, Nucl. Instrum. Meth. **A 595** (2008) 270.

[12] http://www.srim.org/.

[13] http://web-docs.gsi.de/w̃eick/atima/.

[14] J. Ruzicka et al., *Investigation of possible applications of Cherenkov technique to measure average energy of beams of relativistic Au-197 nuclei in energy range 0.64-GeV/u to 0.99-GeV/u*, Nucl. Instrum. Meth. **A 369** (1996) 23.

[15] J. Ruzicka et al., *The Vavilov-Cherenkov radiation arising at deceleration of heavy ions in a transparent medium*, *Nucl. Instrum. Meth.* **A 431** (1999) 148.

[16] J. Ruzicka et al., *Vavilov-Cherenkov radiation emitted by heavy ions near the threshold*, *Vacuum* **63** (2001) 591.

[17] M. Machida et. al, *Development of Ring-imaging Cherenkov Counter for Heavy Ions*, PoS(INPC2016)084.

[18] *GSI Scientific report 2016*, GSI Report 2017–1 (2017) [DOI:10.15120/GR-2017-1].

2018 JINST 13 C02015